International Journal of Power Electronics and Drive System (IJPEDS)
Vol. 16, No. 2, June 2025, pp. 808~816
ISSN: 2088-8694, DOI: 10.11591/ijpeds.v16.i2.pp808-816

DTC of PMSM based on a simple duty ratio approach with ripple reduction scheme

Berhanu Deggefa Lemma[1], Srinivasan Pradabane[2], Tole Sutikno[3], Getu Girma Reta[4], Negasa Muleta Feyisa[1]
[1]College of Electrical and Computer Engineering, Dire Dawa University, Dire Dawa, Ethiopia
[2]Department of Electrical Engineering, National Institute of Technology Warangal, Warangal, India
[3]Department of Electrical Engineering, Faculty of Industrial Technology, Universitas Ahmad Dahlan, Yogyakarta, Indonesia
[4]College of Mechanical and Industrial Engineering, Dire Dawa University, Dire Dawa, Ethiopia

Article Info

Article history:

Received Oct 1, 2024
Revised Apr 1, 2025
Accepted May 6, 2025

Keywords:

Direct torque control
Duty ratio
Four-quadrant ripple
PMSM
SVPWM

ABSTRACT

Today, phase permanent magnet synchronous motor (PMSM) applies to electric drives. But due to its structure and control scheme, PMSM suffers from ripple performance when a control scheme like direct torque control (DTC) is used. This work uses a simple scheme to generate switching signals and determine duty ratios. The duty ratio is obtained from the Volt-second balance. Switching signal generation is performed in the DTC scheme by incorporating the effects of duty ratio, torque error, flux error, and sector number. Dwelling time is obtained in volt-seconds using the reference voltage magnitude and sector number. But voltage state selection is done using the DTC lookup table. Since the DTC lookup table is used for voltage state selection only one active and one null voltage is used. Both active and null voltage periods are divided into two parts and each voltage vector is applied twice in one total switching period. The proposed scheme is tested in MATLAB 2021b. Simulation results indicate that the method is effective in terms of dynamics and harmonics. The scheme torque ripple is 12.5%. Likewise, the flux ripple and harmonic are 0.69% and 0.79%, respectively. Additionally, the scheme is effective for both four quadrants and wide-speed operation. Verification of the proposed scheme is done with OPAL-RT (OP4500). The scheme appears to be effective.

Corresponding Author:

Berhanu Deggefa Lemma
College of Electrical and Computer Engineering, Dire Dawa University
Dire Dawa, Ethiopia
Email: bezakiyya@gmail.com

1. INTRODUCTION

In drive applications, a fast dynamic response is required to respond on time to any external disturbance. It is recommended to use direct torque control whenever a fast response is required [1], [2]. A direct torque control (DTC) algorithm results in significant torque ripples when applied to phase permanent magnet synchronous motor (PMSM) [3]-[6]. Field weakening is integrated into DTC for PMSM control in [7]. This control scheme is recommended when driving a motor above its rated speed. It was mentioned in [8] that an adaptive model can improve ripple performance compared to conventional DTC. Extended finite duty reduces torque and flux fluctuations [9]. It is possible to achieve multiple voltage outputs using a midpoint saturation controller [10]. Saturation controllers improve steady-state response. According to [11], torque ripple can be reduced without trust and flux gain tuning. To obtain the fastest dynamic response and optimal steady state, a duty ratio based on root mean squared error minimization is applied to determine a duty ratio for optimal torque ripple reduction [12].

The [13], [14], the duty ratio is computed to minimize torque and flux ripple. An easy method for computing the duty ratio that only considers torque and speed errors is presented in [15]. Fixed switching pulse width modulation (PWM)-based DTC is forwarded for the PMSM drive in [16]. The duty cycle optimization is performed by taking the sum of actual changes due to applied voltage and setting it equal to an error. Duty ratio manipulation of DTC based on a PMSM drive supplied by a hybrid voltage vector was proposed in [17]. A hybrid vector is supplied according to the subsector within the conventional sector. The conventional sector is divided into five subsectors and different voltage combinations are selected for each subsector. Duty is computed as the ratio of error to maximum compensation obtained when voltage is applied for the entire period. Optimal voltage-based DTC for a brushless DC motor is presented in [18]. The main disadvantage of this work is high harmonics, which significantly impact the drive system. The lookup table was replaced with fuzzy logic to include the magnitude of the error and the sign of the error [19]. This method has a better response than conventional direct torque control because it applies different vectors for different levels of error. But in this scheme, also one vector stays for the whole period once it is applied based on the given criteria. The work in [20] presents a novel control strategy for a five-phase permanent magnet synchronous motor (5P-PMSM) focusing on sensorless speed regulation. It integrates a genetic algorithm (GA) with a backstepping control method to optimize system performance.

The work incorporates the GA to determine the best control gains, addressing the limitations of traditional empirical tuning methods and sliding model observer to estimate the electromotive force, rotor position, and motor speed, reducing the need for physical sensors and enhancing system reliability. The work presented in [21], discusses the analytical design of self-sensing control (SSC) for PMSM using a quasi-direct (QD) calculation method. The focus is on simplifying the commissioning of SSC systems, making them more accessible for a wider range of applications. The work in [22] presents a novel method for controlling PMSM using a compensated duty ratio optimized DTC scheme. The primary aim is to reduce the ripple magnitude in the developed torque, which is a common issue in conventional DTC systems. The work presented in [23] focus on the high fidelity and computational efficiency of the finite-element analysis (FEA)-based model to present a performance prediction strategy for DTC of PMSM under different pulse selectors. The work presented in [24] focus on a novel sliding band for torque and flux hysteresis controllers to improve the current total harmonic distortion (THD) with a special focus on low-speed regions. The proposed DTC schemes offer smooth low-speed operation with only a marginal increase in switching frequency. The work in [25] presents the model predictive control direct torque control (MC-DTC) method that employs residual vectors (RVs). Whereas the work presented by [26], focuses on deadbeat control theory, offering improved steady-state and transient performance for PMSM drives by minimizing stator current ripples and optimizing torque dynamics. By employing a novel maximum torque per ampere (MTPA) based reference calculation and reducing computational complexity. Whereas the work in [27] presents a proportional-plus-integral resonant (PI-RES) controller-based model predictive control (MPC) approach for PMSM drives, effectively minimizing torque ripples and improving current control performance.

This paper presents a method to determine duty ratios without optimizing the cost function. By using this method, the duty ratio is calculated without the slope. In this work, the opposite of DTC-SVPWM is performed. In DTC-SVPWM, torque and flux error are used for reference voltage generation. The control signal is generated from dwelling time computed using a volt-second balance. This work uses the reference from the controller output and feedforward for calculating dwelling time. Taking the dwelling time, a sign of torque error, a sign of flux error, and flux sector number, the switching signal is generated. Only one active voltage is used in this method. The null voltage is applied in such a way that the number of commutations is low. The same active voltage is used in a two-interval gap.

2. METHOD

The proposed system consists of four main components: the switching signal processing unit, inverter, motor, and feedback system, each playing a crucial role in ensuring efficient motor control. The switching signal processing unit is responsible for generating accurate control signals to drive the inverter. This process begins with the computation of dwelling time, which determines how long each switch in the inverter remains active within a switching cycle. Using this dwelling time, the duty ratio is then calculated, controlling the pulse width of the switching signals for precise modulation. To ensure real-time accuracy, the torque error is computed by comparing the actual motor torque with the reference torque, enabling dynamic adjustments. Similarly, the flux error is determined by evaluating the deviation between the measured flux and its reference value, ensuring efficient energy use and stable operation. Another essential step is the determination of the flux sector, which identifies the rotor flux vector's position within predefined sectors, guiding the selection of appropriate voltage vectors in the inverter. Finally, the switching signals are generated based on the computed duty ratio, sector number, flux error, and torque error, ensuring that the inverter applies the correct voltage and current to the motor. This coordinated control strategy optimizes motor performance, enhances stability, and enables a robust closed-loop system for precise speed and torque regulation. This can be seen in Figure 1.

The details of switching signal generation and the rationale behind this work are explained in the diagram depicted in Figure 2. The diagram in Figure 2(a) indicates the scheme used for signal generation, whereas the diagram depicted in Figure 2(b) indicates the comparison of conventional DTC, duty ratio optimized DTC, and the one proposed in this work. The legend for this picture is given in a diagram depicted in Figure 2(b). This function generates switching signals based on torque error, flux error, sector number, and time span indicators. It begins by initializing all signals to zero and then assigns specific values according to predefined conditions. This process effectively implements sector-based switching logic for motor control, ensuring optimal performance by adapting switching states to different operating conditions. The time span is divided to apply active and null voltages twice within a single switching period. Table 1 defines the switching logic and selects the appropriate null voltage based on the state of the active voltage.

The dwelling time is obtained from the control signal when Vdff and Vqff are direct and quadrature axis feedforward voltage magnitudes. The switching time for active voltage is obtained as the sum of T_1 and T_2, when T_1 and T_2 are switching states for the first active voltage and the second active voltage. $Vref$ is the reference voltage and T_s is the total switching period.

$$\begin{cases} T_1 = \dfrac{3 \times Vref \times T_s \times sin(3-\theta)}{Vdc \times sin(\frac{pi}{3})} \\ T_2 = \dfrac{3 \times Vref \times T_s \times sin(\theta - \frac{(n-1)pi}{3})}{Vdc \times sin(\frac{pi}{3})} \end{cases} \tag{1}$$

The value of T_0 is obtained by subtracting the active voltage time from the total switching period. The expression depicted below shows the simple way to determine the duty ratio.

$$D = \frac{T_1 + T_2}{T_s} \tag{2}$$

A conventional direct torque control considers only torque and flux error when generating switching signals. The simple lookup table for conventional direct torque control is shown in Table 1.

Table 1. Conventional lookup table

Δψ	ΔT	Sector number					
		1	2	3	4	5	6
1	1	V2(110)	V3	V4	V5	V6	V1
	0	V0(000)	V7	V0	V2	V0	V2
	-1	V6(101)	V1(100)	V2	V3	V4	V5
0	1	V3(010)	V4(011)	V5	V6	V1	V2
	0	V7(111)	V0	V7	V0	V7	V0
	-1	V5(001)	V6	V1	V2	V3	V4

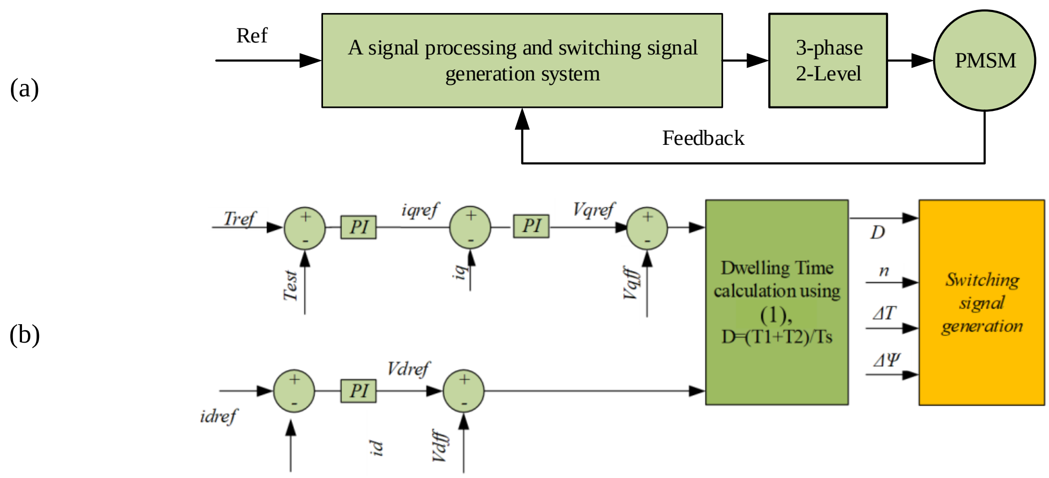

Figure 1. Illustrates the overall layout and operating principle of the proposed system, where (a) shows the proposed scheme and (b) shows the duty ratio determination and switching signal generation

(a)

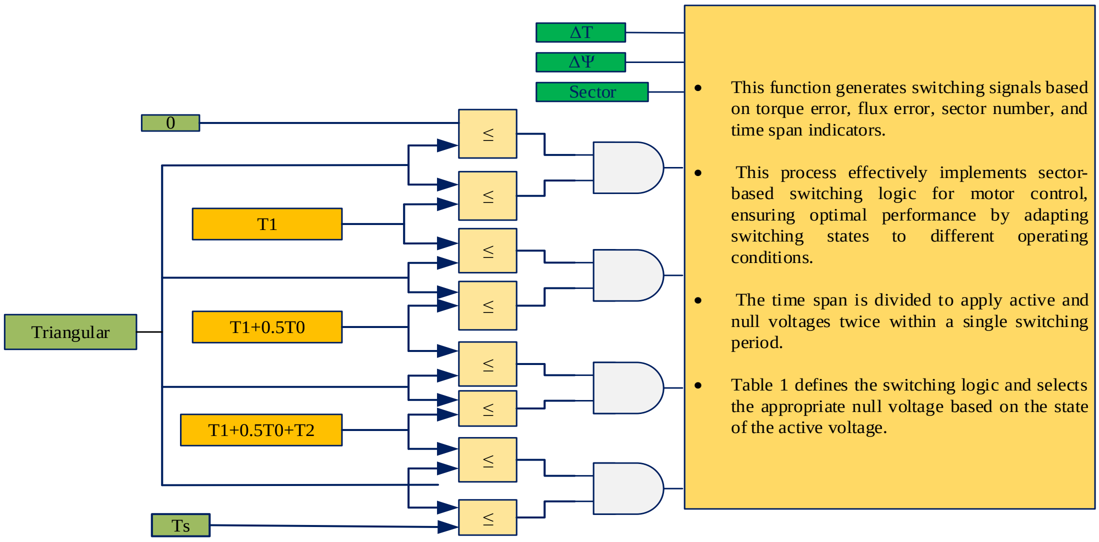

(b)

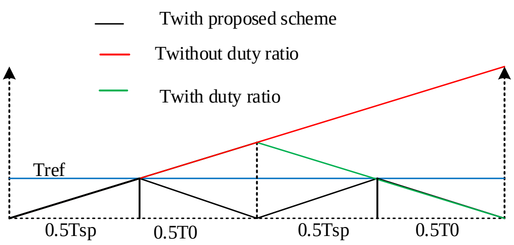

Figure 2. Shows the details of switching signal generation and comparison of DTC when (a) shows switching signal generation and (b) shows the comparison of DTC in different active and null voltage combinations

As it is shown in Table 1, based on the sign of the error of torque and flux voltage state is selected. But the one voltage states are applied throughout the switching period. This increases the ripple magnitude. In this section, the on-time for active voltage is obtained from the dwell time. The switching signal is generated using the sector number, torque error, flux error, and duty ratio. The duty ratio is translated into time, and the switching signal is generated based on these four parameters. In addition to the four parameters mentioned here, the total switching period is divided into four parts. A time span is determined by using the four logic AND gates shown in Figure 2. Based on the torque error, flux error, sector number, and time, the voltage state is applied. For instance, if the ΔT is positive, Δψ is zero, and the sector number is six, the voltage state is selected based on the time span. For case mentioned above, for the time span 0→T1, T1→T1+0.5T0, T1+0.5T0→T1+T2+0.5T0, and T1+T2+0.5T0→Ts, voltage state is V2(110), V7(111), V2(110) and V7(111) respectively. For the period from 0→0.5Tsp, the active voltage is applied, whereas for the time from 0.5Tsp→0.5T0+0.5Tsp, the null voltage is used. In the same fashion, for the time from 0.5T0+0.5Tsp→Tsp+0.5T0, active voltage is applied. Whereas for the last span for the time from Tsp+0.5T0→Ts, the null voltage is used. The advantage of this scheme is reducing the effect of inertial forces. The null voltage is selected based on the scheme that enhances the reduction of the commutation number. Both voltages are applied twice in one switching period. This scheme is employed to reduce the ripple level. Figure 2(b) depicts the advantages of the scheme assuming T1 = T2 and Tsp is the sum of T1 and T2. As the number of partitions increases, the level of torque ripple decreases. For specific n, ΔΨ, and ΔT, when n represents sector number, ΔΨ, and ΔT are errors in flux and torque; the voltage is used in the sequence depicted in Figure 2(b), shown in black color. A line in red in Figure 2(b) indicates the torque response without a duty ratio, and a line in green indicates the torque response with a duty ratio. The black color line shows when both active and null voltages are applied twice by dividing the time into two parts.

3. RESULTS AND DISCUSSION

MATLAB 2021b is used for simulation, with data from Table 2. Figure 3 shows results at constant speed and torque, evaluating steady-state performance. In the simulation, to see the dynamics and steady-state performance, the reference speed and load torque were kept at is kept at 752 rpm and 5 Nm, and the simulation was done.

Table 2. Data used in the simulation

Parameter	Magn	Parameter	Magn
Inductance	10.5 mH	Magnet flux	0.725 Wb
Frequency	10 kHz	Rated current	10 A
Resistance	1.12 ohm	power	3.7 kW
Pole pair	4	speed	1500 rpm

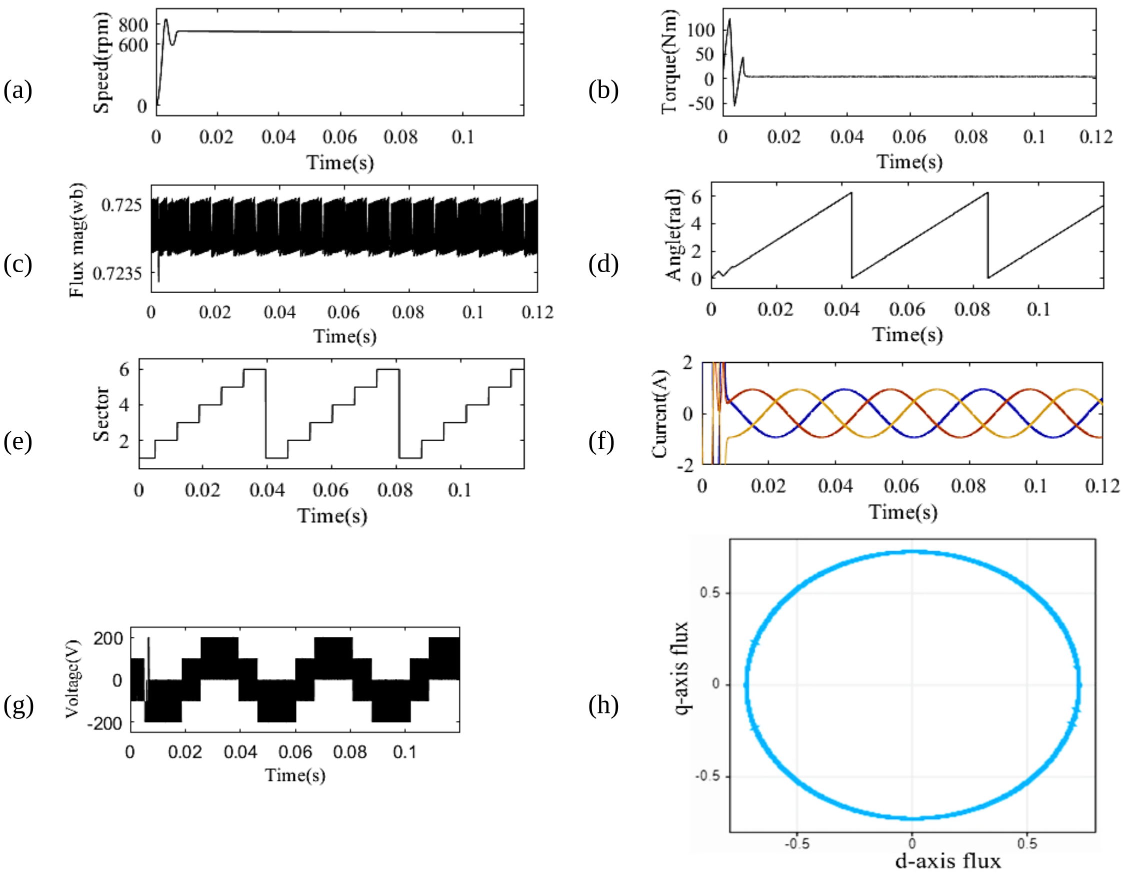

Figure 3. Steady-state performance of the proposed scheme: (a) speed response, (b) torque response, (c) flux magnitude, (d) flux angle, (e) sector number, (f) current waveform, (g) voltage waveform, and (h) flux plot

Figure 3 illustrates the steady-state performance of the proposed scheme. The speed response (Figure 3(a)), torque response (Figure 3(b)), and flux magnitude (Figure 3(c)) are shown along with the flux angle (Figure 3(d)) and sector number (Figure 3(e)). Figures 3(f) and 3(g) display the current and voltage waveforms, while Figure 3(h) provides the flux plot, collectively representing the system's behavior under steady-state conditions. The rise time for the speed is $3.5\text{x}10^{-3}$ seconds, whereas the settling time is $7\text{x}10^{-3}$ seconds. An overshoot is 16%. The ratio of ripple from reference to maximum deviation can be used to represent ripple performance. When Δ maximum deviation from the reference.

$$T_{ripple}\% = \frac{0.5\Delta}{0.5(T\,min + T\,max)} \times 100 \tag{3}$$

PMSM is mostly used in applications where speed reversal is required. Depending on the situation, torque may be applied. The results shown in Figure 4 are taken to assess the effectiveness of the proposed scheme for four-quadrant operation. The speed and torque were kept constant, and the direction of motion and sign of load torque were changed to see the performance in all four quadrants.

The diagrams in Figure 4(a) to Figure 4(i) were drawn by taking the simulation at different speed levels. The speed is varied from 250 to 1000, and the mentioned variables were calculated. A power loss ratio is calculated by dividing harmonic current loss by total current loss.

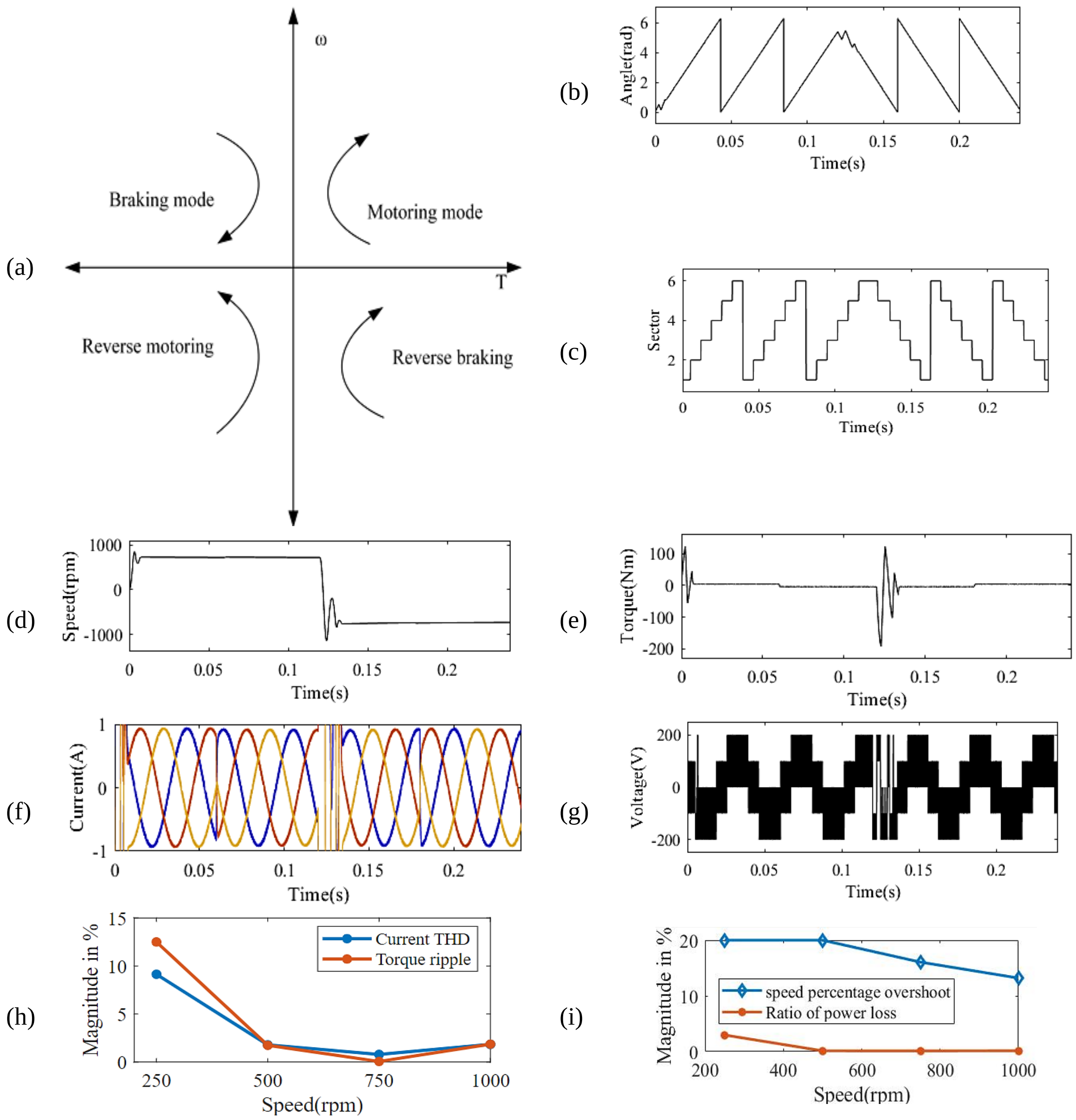

Figure 4. Shows the four quadrant operation of PMSM with a proposed control scheme: (a) four quadrant operation of the motor, (b) flux angle, (c) flux sector, (d) speed, (e) torque, (f) current, (g) voltage, (h) torque ripple and current harmonic performance, and (i) percentage of speed overshoot and harmonic power loss to total active power loss

4. EXPERIMENTAL VERIFICATION

Hardware-in-the-loop (HIL) simulation is a powerful technique used to evaluate the efficiency of control methods by integrating real-time hardware with software-based simulations. This approach enables rigorous validation and testing of control algorithms under realistic operating conditions before deploying them in real-world applications. Figure 5(a) illustrates the HIL system layout, which consists of the OPAL-RT OP4500 real-time simulator and a desktop computer. The OP4500 serves as the core computational unit, capable of running high-fidelity simulations while interfacing with external controllers. The desktop computer is responsible for monitoring, configuring, and analyzing the simulation results in real time. The results obtained from the HIL system, as shown in Figures 5(b) to 5(e), demonstrate the system's response under specific operating conditions. The experimental setup was subjected to a load torque of 8 Nm while maintaining a rotational speed of 752 rpm. The results depicted in Figure 5, according to (3), the magnitude of ripple for speed and flux is 0.265 and 1.37 %, respectively. This indicates that the speed and flux ripple are small. Additionally, the current, voltage, and flux waveforms are distortion-free.

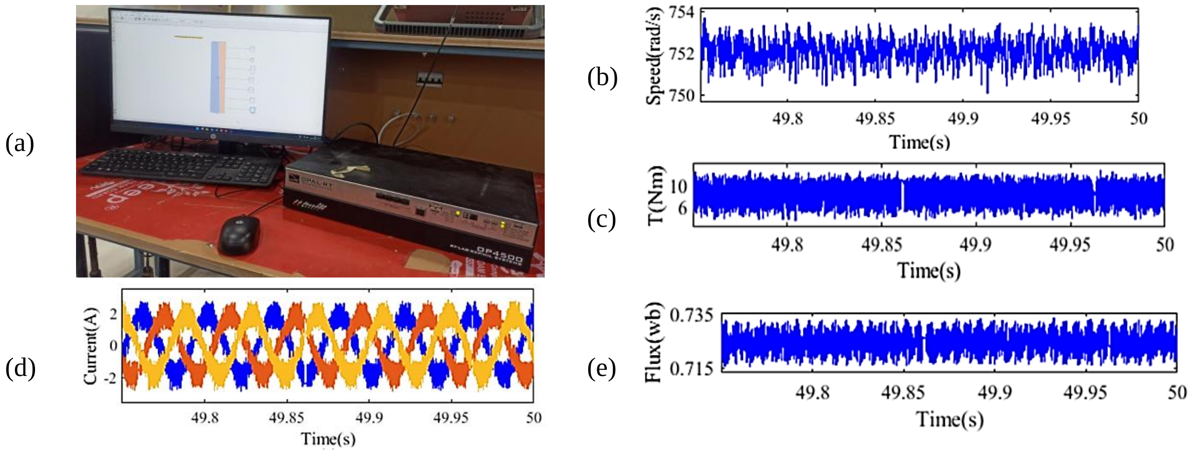

Figure 5. Shows the real-time simulation scheme when (a) real-time simulator, (b) speed response, (c) torque response, (d) current, and (e) flux magnitude

5. CONCLUSION

A simple and improved DTC scheme for PMSM was proposed in this study. Both duty ratio determination and switching signal generation are simple in this scheme. The duty ratio is calculated from the Volt-second balance principle for space vector pulse width modulation. DTC schemes generate switching signals by incorporating duty ratio effects into the switching signal generation. According to the results, the scheme performs well. In addition, the scheme is effective for four quadrants, variable torque, and speed operation. The hardware result also proves the effectiveness of the proposed scheme.

ACKNOWLEDGMENTS

We express our gratitude to Dire Dawa University for permitting us to utilize the available laboratory equipment for this project. However, we did not receive any funds for this work.

FUNDING INFORMATION

There is no fund is received for this work.

AUTHOR CONTRIBUTIONS STATEMENT

This journal uses the Contributor Roles Taxonomy (CRediT) to recognize individual author contributions, reduce authorship disputes, and facilitate collaboration.

Name of Author	C	M	So	Va	Fo	I	R	D	O	E	Vi	Su	P	Fu
Berhanu Deggefa Lemma	✓	✓	✓	✓	✓	✓		✓	✓	✓	✓			
Srinivasan Pradabane	✓			✓			✓		✓	✓	✓	✓	✓	
Tole Sutikno	✓									✓				✓
Getu Girma Reta	✓									✓				
Negasa Muleta Feyisa	✓									✓				

C : **C**onceptualization
M : **M**ethodology
So : **So**ftware
Va : **Va**lidation
Fo : **Fo**rmal analysis
I : **I**nvestigation
R : **R**esources
D : **D**ata Curation
O : Writing - **O**riginal Draft
E : Writing - Review & **E**diting
Vi : **Vi**sualization
Su : **Su**pervision
P : **P**roject administration
Fu : **Fu**nding acquisition

CONFLICT OF INTEREST STATEMENT

This article is our original work, and the contributions of each author are specified using the Contributor Roles Taxonomy (CRediT). The authors declare that there are no conflicts of interest.

DATA AVAILABILITY

The data that support the findings of this study are available from the corresponding author, [BD], upon reasonable request.

REFERENCES

[1] A. Nyitrai, G. Szabó, and S. R. Horváth, "Parameter determination and drive control analysis of axial flux permanent magnet synchronous motors," *Periodica Polytechnica Electrical Engineering and Computer Science*, vol. 66, no. 2, pp. 205–214, May 2022, doi: 10.3311/PPee.19714.

[2] M. Zigliotto, "Permanent magnet synchronous motor drives," in *Power Electronic Converters and Systems: Frontiers and Applications*, 2015, pp. 313–332. doi: 10.1049/PBPO074E_ch10.

[3] Q. Wang, H. Yu, M. Wang, and X. Qi, "An improved sliding mode control using disturbance torque observer for permanent magnet synchronous motor," *IEEE Access*, vol. 7, pp. 36691–36701, 2019, doi: 10.1109/ACCESS.2019.2903439.

[4] K. Li and Y. Wang, "Maximum torque per ampere (MTPA) control for IPMSM drives using signal injection and an MTPA control law," *IEEE Transactions on Industrial Informatics*, vol. 15, no. 10, pp. 5588–5598, Oct. 2019, doi: 10.1109/TII.2019.2905929.

[5] Z. Zhang, G. Li, Z. Qian, Q. Ye, and Y. Xia, "Research on effect of temperature on performance and temperature compensation of interior permanent magnet motor," in *2016 IEEE 11th Conference on Industrial Electronics and Applications (ICIEA)*, IEEE, Jun. 2016, pp. 411–414, doi: 10.1109/ICIEA.2016.7603619.

[6] K.-K. Shyu, J.-K. Lin, V.-T. Pham, M.-J. Yang, and T.-W. Wang, "Global minimum torque ripple design for direct torque control of induction motor drives," *IEEE Transactions on Industrial Electronics*, vol. 57, no. 9, pp. 3148–3156, Sep. 2010, doi: 10.1109/TIE.2009.2038401.

[7] M. F. Rahman, L. Zhong, and K. W. Lim, "A direct torque-controlled interior permanent magnet synchronous motor drive incorporating field weakening," *IEEE Transactions on Industry Applications*, vol. 34, no. 6, pp. 1246–1253, 1998, doi: 10.1109/28.738985.

[8] Y. A.-R. I. Mohamed, "A newly designed instantaneous-torque control of direct-drive PMSM servo actuator with improved torque estimation and control characteristics," *IEEE Transactions on Industrial Electronics*, vol. 54, no. 5, pp. 2864–2873, Oct. 2007, doi: 10.1109/TIE.2007.901356.

[9] C. Xia, S. Wang, X. Gu, Y. Yan, and T. Shi, "Direct torque control for VSI-PMSM using vector evaluation factor table," *IEEE Transactions on Industrial Electronics*, vol. 63, no. 7, pp. 4571–4583, Jul. 2016, doi: 10.1109/TIE.2016.2535958.

[10] Z. Zhang, C. Wei, W. Qiao, and L. Qu, "Adaptive saturation controller-based direct torque control for permanent-magnet synchronous machines," *IEEE Transactions on Power Electronics*, vol. 31, no. 10, pp. 7112–7122, 2016, doi: 10.1109/TPEL.2015.2511073.

[11] M. A. M. Cheema, J. E. Fletcher, D. Xiao, and M. F. Rahman, "A direct thrust control scheme for linear permanent magnet synchronous motor based on online duty ratio control," *IEEE Transactions on Power Electronics*, vol. 31, no. 6, pp. 4416–4428, Jun. 2016, doi: 10.1109/TPEL.2015.2475400.

[12] M. H. Vafaie, B. Mirzaeian Dehkordi, P. Moallem, and A. Kiyoumarsi, "A new predictive direct torque control method for improving both steady-state and transient-state operations of the PMSM," *IEEE Transactions on Power Electronics*, vol. 31, no. 5, pp. 3738–3753, May 2016, doi: 10.1109/TPEL.2015.2462116.

[13] M. H. Vafaie, B. M. Dehkordi, P. Moallem, and A. Kiyoumarsi, "Improving the steady-state and transient-state performances of PMSM through an advanced deadbeat direct torque and flux control system," *IEEE Transactions on Power Electronics*, vol. 32, no. 4, pp. 2964–2975, Apr. 2017, doi: 10.1109/TPEL.2016.2577591.

[14] Z. Zhang and X. Liu, "A duty ratio control strategy to reduce both torque and flux ripples of DTC for permanent magnet synchronous machines," *IEEE Access*, vol. 7, pp. 11820–11828, 2019, doi: 10.1109/ACCESS.2019.2892121.

[15] F. Niu *et al.*, "A simple and practical duty cycle modulated direct torque control for permanent magnet synchronous motors," *IEEE Transactions on Power Electronics*, vol. 34, no. 2, pp. 1572–1579, Feb. 2019, doi: 10.1109/TPEL.2018.2833488.

[16] S. J. Kim, J.-W. Kim, B.-G. Park, and D.-H. Lee, "A novel predictive direct torque control using an optimized PWM approach," *IEEE Transactions on Industry Applications*, vol. 57, no. 3, pp. 2537–2546, May 2021, doi: 10.1109/TIA.2021.3060693.

[17] T. Yuan, D. Wang, X. Wang, X. Wang, and Z. Sun, "High-precision servo control of industrial robot driven by PMSM-DTC utilizing composite active vectors," *IEEE Access*, vol. 7, pp. 7577–7587, 2019, doi: 10.1109/ACCESS.2018.2890539.

[18] S. Dangeam, "Three-phase inverter with direct torque control for a brushless DC motor," *ECTI Transactions on Electrical Engineering, Electronics, and Communications*, vol. 20, no. 1, pp. 133–142, Feb. 2022, doi: 10.37936/ecti-eec.2022201.246118.

[19] S. L. Belaid, "Improved IM DTC by using a fuzzy switching table in PV applications," *Elektrotehniski Vestnik/Electrotechnical Review*, vol. 88, no. 1–2, pp. 26–32, 2021.

[20] H. H. Boughezala, K. Laroussi, S. Khadar, A. S. Al-Sumaiti, and M. A. Mossa, "Optimized sensorless control of five-phase permanent magnet synchronous motor using a genetic algorithm-real time implementation," *IEEE Access*, vol. 12, pp. 98367–98378, 2024, doi: 10.1109/ACCESS.2024.3429181.

[21] N. Himker and A. Mertens, "Analytical design of self-sensing control for PMSM using quasi-direct calculation," *IEEE Open Journal of Industry Applications*, vol. 4, pp. 149–159, 2023, doi: 10.1109/OJIA.2023.3276820.

[22] B. D. Lemma and S. Pradabane, "Control of PMSM drive using lookup table based compensated duty ratio optimized direct torque control (DTC)," *IEEE Access*, vol. 11, pp. 19863–19875, 2023, doi: 10.1109/ACCESS.2023.3249111.

[23] A. Nasr *et al.*, "Performance prediction of direct torque-controlled PMSM drives considering different pulse selectors using FEA-based model," *IEEE Open Journal of Power Electronics*, vol. 4, pp. 687–702, 2023, doi: 10.1109/OJPEL.2023.3311951.

[24] A. Mohan, M. Khalid, and A. C. Binojkumar, "A novel sliding hysteresis band based direct torque control scheme for PMSM motors to achieve improved current THD with reduction in torque and flux ripples eliminating the low-speed problems," *IEEE Access*, vol. 12, pp. 67971–67985, 2024, doi: 10.1109/ACCESS.2024.3400684.

[25] W. Deng, J. Tang, and W. Cheng, "An enhanced rotating vector-based direct torque control for matrix converter-fed PMSM drives using virtual pulsating vectors," *CPSS Transactions on Power Electronics and Applications*, vol. 8, no. 1, pp. 65–73, Mar. 2023, doi: 10.24295/CPSSTPEA.2023.00007.

[26] S. Shukla, M. Sreejeth, and M. Singh, "Minimization of ripples in stator current and torque of PMSM drive using advanced predictive current controller based on deadbeat control theory," *Journal of Power Electronics*, vol. 21, no. 1, pp. 142–152, Jan. 2021, doi: 10.1007/s43236-020-00151-2.

[27] Suryakant, M. Sreejeth, M. Singh, and A. K. Seth, "Minimization of torque ripples in PMSM drive using PI- resonant controller-based model predictive control," *Electrical Engineering*, vol. 105, no. 1, pp. 207–219, Feb. 2023, doi: 10.1007/s00202-022-01660-y.

BIOGRAPHIES OF AUTHORS

Berhanu Deggefa Lemma was born in Diksis, Ethiopian 1988. He received his B.Sc. and M.Sc. from Adama Science and Technology University in 2012 and 2017 respectively, and his Ph.D. in September 2023 from National Institute of Technology Warangal. He has published journal in IEEE and presented a paper at the international conference. He is working on an electric drive and power electronics. He can be contacted at email: bezakiyya@gmail.com or berhanu.deggefa@ddu.edu.et.

Srinivasan Pradabane was born in Pondicherry, India 1983. He received his graduate degree from Pondicheny University in 2005 and his post-graduate degree from Anna University in 2008. He received his Ph.D. from NITW in 2016. He did his post-doctoral research in the United Kingdom in 2021. He published many articles in reputable journals. His research interests include multilevel inverters, WM schemes, induction motor drives, electric vehicles, integration of renewable energy, DC motor drives, BLDC drives, PMSM drives, LIM drives, propulsion technology for vehicles, measurement techniques, open-end winding drives, driver circuits, and digital control. He can be contacted at email: spradabane@nitw.ac.in.

Tole Sutikno is a lecturer and the head of the master program of Electrical Engineering at the Faculty of Industrial Technology at Universitas Ahmad Dahlan (UAD) in Yogyakarta, Indonesia. He received his bachelor of engineering from Universitas Diponegoro in 1999, master of engineering from Universitas Gadjah Mada in 2004, and doctor of philosophy in Electrical Engineering from Universiti Teknologi Malaysia in 2016. All three degrees are in Electrical Engineering. He has been a Professor at UAD in Yogyakarta, Indonesia, since July 2023, following his tenure as an associate professor in June 2008. He is the Editor-in-Chief of TELKOMNIKA and head of the Embedded Systems and Power Electronics Research Group (ESPERG). He is one of the top 2% of researchers worldwide, according to Stanford University and Elsevier BV's list of the most influential scientists from 2021 to the present. His research interests cover digital design, industrial applications, industrial electronics, industrial informatics, power electronics, motor drives, renewable energy, FPGA applications, embedded systems, artificial intelligence, intelligent control, digital libraries, and information technology. He can be contacted at email: tole@te.uad.ac.id.

Getu Girma Reta was born in Arsi, Ethiopian 1989. He received his B.Sc. and M.Sc. from Dire Dawa and Addis Ababa University in 2014 and 2018, respectively. His research area is optimization techniques for manufacturing, supply chain management system, product optimization, product design, facility and system layout, and quality system management. He publishes more than 5 journals and 2 books. He can be contacted at email: getuie21@gmail.com.

Negasa Muleta Feyisa was born in 1987. He has got his B.Sc. and M.Sc. from Adama Science and Technology University, Ethiopia, in 2012 and 2016, respectively, with specialization in Electrical Power Engineering. He got his Ph.D. from NIT Warangal, India, in 2023. His research area is optimization of hybrid renewable energy, power system quality, stability, and real-time power system control and operation. He can be contacted at email: negisha2005@gmail.com.